ANALYTICAL SOLUTION FOR LONG-WAVE SCATTERING BY A SUBMERGED CYLINDER IN AN AXI-SYMMETRICAL PIT

Huan-Wen Liu
School of Sciences, Guangxi University for Nationalities, Nanning, Guangxi, P.R. China., mengtian29@163.com

Xiao-Ling Sun
School of Sciences, Guangxi University for Nationalities, Nanning, Guangxi, P.R. China.

ANALYTICAL SOLUTION FOR LONG-WAVE SCATTERING BY A SUBMERGED CYLINDER IN AN AXI-SYMMETRICAL PIT

Acknowledgements

ANALYTICAL SOLUTION FOR LONG-WAVE SCATTERING BY A SUBMERGED CYLINDER IN AN AXI-SYMMETRICAL PIT

Huan-Wen Liu and Xiao-Ling Sun

ABSTRACT

This paper proposes an analytical solution to the long-wave equation for waves propagating over a submerged cylinder located in a pit. The pit was assumed to be axi-symmetrical and convex or concave in shape, which may represent a submerged sill being scoured at its toe. Techniques of variable separation and Taylor series expansion were applied to find the analytical solution. It is found that Longuet-Higgins' classical analytical solutions for waves scattered by a submerged circular sill and by a submerged circular pit are actually special cases of the present analytical solution. By using this analytical solution, the influence of the incident wavelength and shape of the pit, including the depth and width, on wave pattern was analysed.

I. INTRODUCTION

Surface gravity waves propagating from the deep ocean to coastal regions may be substantially amplified by reflection, refraction, diffraction, and shoaling because of variation in water depth. Analytical solutions are particularly favorable in studies on wave scattering because of their high accuracy, low cost in labour, and timesaving; however, they are obtainable for only special topographies and simple governing equations.

Regarding three-dimensional bathymetries, several analytical solutions to the long-wave equation have been determined for wave scattering by axi-symmetrical topographies, such as a circular cylindrical island mounted on a paraboloidal shoal [1], conical island and a circular paraboloidal shoal [21], circular cylindrical island mounted on a conical shoal [22], circular cylindrical island mounted on a general shoal [20],

circular paraboloidal pit [19], truncated general shoal [8], circular general pit [6], circular island [4], circular general hump [11, 15], dredge excavation pit [16], vertical cylinder containing an idealised scour pit [17], circular island consisting of combined topographies [3], and circular island mounted on a general shoal [12].

In 2004, approximate analytical solutions to the mild-slope equation were developed by Liu *et al.* [10] for wave scattered by a circular cylindrical island mounted on a paraboloidal shoal, and then extended by Lin and Liu [7], Liu and Lin [9], Jung and Suh [5], Hsiao *et al.* [2], and Niu and Yu [18] for wave scattered by other axi-symmetrical bathymetries.

In this paper, we studied linear long wave scattering by a submerged circular cylinder mounted on an axi-symmetrical pit, which may represent a submerged sill being scoured at its toe. An analytical solution in the form of Taylor series to the long-wave equation is detailed in Section II. Section III presents computational results and related discussion. When the width or the depth of the pit becomes markedly short, the present solution can degenerate into the classical analytical solution for wave scattered by a submerged circular sill or pit developed by Longuet-Higgins [13]. According to the proposed solution, the influence of both pit depth and width and the incident wave period on the wave pattern was investigated.

II. SOLUTION TECHNIQUE

We focused on a scattering problem of simple harmonic waves over a submerged cylinder containing an axi-symmetrical pit (see Fig. 1). Assume that a is the radius of the cylinder, b is the distance from the pit centre to the actual edge of the pit, c is the radial distance from the pit centre to the imaginary edge of the pit extended to the water surface, h_0 is the water depth in the region outside the pit, h_1 is the water depth over the cylinder, h_a is the water depth along the cylinder, and h_c is the distance between the crest of the pit and the stagnant sea level. Let the origin of the horizontal coordinate system be the vertical projection of the centre of the pit in the stagnant water surface. The water depth varies along the radial direction as follows:
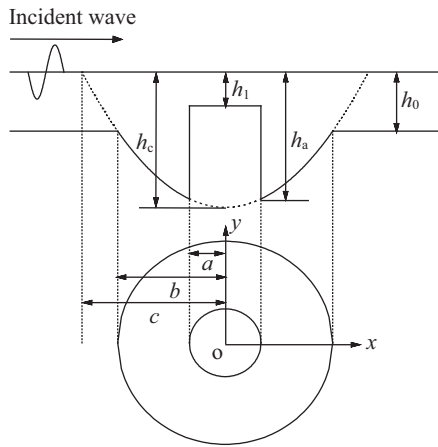
Fig. 1. Definition sketch of a submerged cylinder containing an axisymmetrical pit.

$$h(r) = \begin{cases} h_0, & b \le r, \\ h_c\left(1 - \dfrac{r^s}{c^s}\right) & a \le r < b, \\ h_1, & r < a, \end{cases} \tag{1}$$

where s is the power exponent that can be an arbitrary positive real number. Thus, the following equation can easily be obtained:

$$\frac{h_c}{h_c - h_0} = \frac{c^s}{b^s}, \; \frac{h_c}{h_c - h_a} = \frac{c^s}{a^s}, \; \frac{h_c - h_0}{h_c - h_a} = \frac{b^s}{a^s}. \tag{2}$$

For convenience, we denote $\mu = -h_c/c^s$; hence, the variable water depth within the pit region can be rewritten as $h(r) = h_c + \mu r^s$.

The long-wave equation for combined refraction and diffraction is expressed as

$$\nabla \cdot (h\nabla \eta) + \frac{\omega^2}{g}\eta = 0, \tag{3}$$

where η is the complex water surface elevation, g is the gravitational acceleration, ω is the wave angular frequency, and ∇ is the horizontal gradient operator.

Because the sea-bottom contours are axi-symmetrical, adopting a cylindrical coordinate system (r, θ) in which $x = r\cos\theta$ and $y = r\sin\theta$ is convenient. Eq. (3) can thus be rewritten as

$$h\left(\frac{\partial^2 \eta}{\partial r^2} + \frac{1}{r}\frac{\partial \eta}{\partial r} + \frac{1}{r^2}\frac{\partial^2 \eta}{\partial \theta^2}\right) + \frac{dh}{dr}\frac{\partial \eta}{\partial r} + \frac{\omega^2}{g}\eta = 0. \tag{4}$$

Furthermore, by expanding $\eta(r, \theta)$ into a Fourier-cosine series

$$\eta(r,\theta) = \sum_{n=0}^{\infty} R_n(r)\cos n\theta, \tag{5}$$

Eq. (4) can be transformed into an ordinary differential equation

$$hr^2 R_n'' + (r^2 h' + hr) R_n' + \left(\frac{\omega^2 r^2}{g} - n^2 h\right) R_n = 0, \; n = 0, 1, 2, \ldots \tag{6}$$

In the outer region with water depth h_0, Eq. (6) degenerates into the Bessel equation

$$R_n'' + \frac{1}{r}R_n' + \left(k_0^2 - \frac{n^2}{r^2}\right)R_n = 0, \tag{7}$$

and the water surface elevation in this region can be written as

$$\eta(r,\theta) = \sum_{n=0}^{\infty}\left[i^n \varepsilon_n J_n(k_0 r) + A_n^{(0)} H_n^{(1)}(k_0 r)\right]\cos n\theta, \tag{8}$$

where the constant coefficient $A_n^{(0)}$ is yet to be determined, $i = \sqrt{-1}$, $k_0 = \omega/\sqrt{gh_0}$, $J_n(k_0 r)$ is the Bessel function of the first kind of order n, $H_n^{(1)}(k_0 r)$ is the Hankel function of the first kind of order n, and ε_n is the Jacobi symbol defined as

$$\varepsilon_n = \begin{cases} 1, & n = 0, \\ 2, & n > 0. \end{cases} \tag{9}$$

In the inner region with constant depth h_1, Eq. (6) degenerates into the Bessel equation

$$R_n'' + \frac{1}{r}R_n' + \left(k_1^2 - \frac{n^2}{r^2}\right)R_n = 0, \tag{10}$$

which in general has two independent particular solutions, namely $J_n(k_1 r)$ and $H_n^{(1)}(k_1 r)$ with $k_1 = \omega/\sqrt{gh_1}$. However, $H_n^{(1)}(k_1 r)$ is singular at $r = 0$ and must be discarded; thus, the general solution to Eq. (10) is simply

$$R_n(r) = A_n^{(1)} J_n(k_1 r), \tag{11}$$

and the water surface elevation in this region is

$$\eta(r,\theta) = \sum_{n=0}^{\infty} A_n^{(1)} J_n(k_1 r)\cos n\theta, \tag{12}$$

in which the constant coefficient $A_n^{(1)}$ must be determined.

In the region of variable water depth, Eq. (6) reads

$$r^2\left(\mu r^s + h_c\right)R_n'' + \left[(s+1)\mu r^{s+1} + h_c r\right]R_n'$$

$$+ \left[\frac{\omega^2 r^2}{g} - n^2\left(\mu r^s + h_c\right)\right]R_n = 0. \qquad (13)$$

In this region, the water depth function $h(r) = h_c + \mu r^s$ is not a power function because $h_c > 0$; in other words, the bathymetry is quasi-idealised. Therefore, the conventional solution technique, which transforms the governing equation into classical equations such as the Euler equation, Bessel equation, or Legendre equation, for determining a closed-form solution used for idealised bathymetries [8, 20, 22] are no longer available, and the technique by means of series expansion must be employed.

Since $r_0 = (a+b)/2$ is an ordinary point to Eq. (13), all the three coefficients in Eq. (13) are analytical functions at r_0 and can thus be expanded into Taylor series at r_0 as follows:

$$r^2\left(\mu r^s + h_c\right) = \sum_{m=0}^{\infty} a_m\left(r - r_0\right)^m, \qquad (14)$$

$$(s+1)\mu r^{s+1} + h_c r = \sum_{m=0}^{\infty} b_m\left(r - r_0\right)^m, \qquad (15)$$

$$\frac{\omega^2 r^2}{g} - n^2\left(\mu r^s + h_c\right) = \sum_{m=0}^{\infty} c_m\left(r - r_0\right)^m, \qquad (16)$$

with

$$a_m = \frac{1}{m!}\left(r^2(\mu r^s + h_c)\right)^{(m)}\Big|_{r=r_0}, \qquad (17)$$

$$b_m = \frac{1}{m!}\left((s+1)\mu r^{s+1} + h_c r\right)^{(m)}\Big|_{r=r_0}, \qquad (18)$$

$$c_m = \frac{1}{m!}\left(\frac{\omega^2 r^2}{g} - n^2\left(\mu r^s + h_c\right)\right)^{(m)}\Big|_{r=r_0}. \qquad (19)$$

A solution to Eq. (13) can then be sought in the form of Taylor series as follows:

$$R_n(r) = A_n^{(2)}U_n(r) + A_n^{(3)}V_n(r)$$

$$= A_n^{(2)}\sum_{l=0}^{\infty} u_{n,l}(r - r_0)^l + A_n^{(3)}\sum_{l=0}^{\infty} v_{n,l}(r - r_0)^l. \qquad (20)$$

Substituting Eqs. (14)-(20) into Eq. (13) obtains

$$u_{n,0} = 1, \quad u_{n,1} = 0, \quad u_{n,2} = -\frac{c_0}{2a_0}, \qquad (21)$$

$$u_{n,l} = -\frac{1}{a_0 l(l-1)}\left(\sum_{j=1}^{l-2}(l-j)(l-j-1)a_j u_{n,l-j}\right.$$

$$\left.+ \sum_{j=0}^{l-2}\left[(l-1-j)b_j u_{n,l-1-j} + c_j u_{n,l-2-j}\right]\right), l = 3, 4, \ldots, \quad (22)$$

$$v_{n,0} = 0, \quad v_{n,1} = 1, \quad v_{n,2} = -\frac{b_0}{2a_0}, \qquad (23)$$

$$v_{n,l} = -\frac{1}{a_0 l(l-1)}\left(\sum_{j=1}^{l-2}(l-j)(l-j-1)a_j v_{n,l-j}\right.$$

$$\left.+ \sum_{j=0}^{l-2}\left[(l-1-j)b_j v_{n,l-1-j} + c_j v_{n,l-2-j}\right]\right), l = 3, 4, \ldots. \quad (24)$$

The complex singularities in Eq. (13), except for $r = 0$, are

$$r_m = \begin{cases} \left(\dfrac{h_a b^s - h_0 a^s}{h_a - h_0}\right)^{\frac{1}{s}} e^{i\frac{2m\pi}{s}}, & m = 0,\ldots,s-1, \ s \text{ is an integer,} \\[4mm] \left(\dfrac{h_a b^s - h_0 a^s}{h_a - h_0}\right)^{\frac{p}{q}} e^{i\frac{2m\pi}{q}}, & m = 0,\ldots,q-1, \ s \text{ is a rational } \dfrac{q}{p}. \end{cases}$$

Furthermore, since

$$\frac{h_a b^s - h_0 a^s}{h_a - h_0} > \frac{h_a b^s - h_0 b^s}{h_a - h_0} = b^s, \qquad (25)$$

the series solution (20) converges for complex r in the disk $|r - r_0| < R$ with

$$R = \min\{|r_0 - 0|, |r_0 - r_m|\} > \min\{r_0, b - r_0\} = (b-a)/2. \qquad (26)$$

Therefore, the series solution (20) converges in the real interval as follows

$$-R + \frac{a+b}{2} = -R + r_0 < r < R + r_0 = R + \frac{a+b}{2} \qquad (27)$$

where $R > (b-a)/2$, which includes the physical interval $[a, b]$ as its subinterval. Finally, the water surface elevation in the variable water depth region is expressed as

$$\eta(r,\theta) = \sum_{n=0}^{\infty}\left(A_n^{(2)}U_n(r) + A_n^{(3)}V_n(r)\right)\cos n\theta$$

$$= \sum_{n=0}^{\infty}\left(A_n^{(2)}\sum_{l=0}^{\infty} u_{n,l}(r - r_0)^l + A_n^{(3)}\sum_{l=0}^{\infty} v_{n,l}(r - r_0)^l\right)\cos n\theta, \qquad (28)$$

where $A_n^{(2)}$ and $A_n^{(3)}$ are constants to be determined.

The continuity of the wave elevations and the flow fluxes at $r = a$ and $r = b$ requires

$$\begin{cases} \eta(r,\theta)\big|_{r=a^-} = \eta(r,\theta)\big|_{r=a^+}, \\ h_1 \dfrac{\partial \eta(r,\theta)}{\partial r}\bigg|_{r=a^-} = h_a \dfrac{\partial \eta(r,\theta)}{\partial r}\bigg|_{r=a^+}, \\ \eta(r,\theta)\big|_{r=b^-} = \eta(r,\theta)\big|_{r=b^+}, \\ \dfrac{\partial \eta(r,\theta)}{\partial r}\bigg|_{r=b^-} = \dfrac{\partial \eta(r,\theta)}{\partial r}\bigg|_{r=b^+}, \end{cases} \tag{29}$$

which is equivalent to

$$\begin{bmatrix} -J_n(k_1 a) & U_n(a) & V_n(a) & 0 \\ -k_1 h_1 J_n'(k_1 a) & h_a U_n'(a) & h_a V_n'(a) & 0 \\ 0 & U_n(b) & V_n(b) & -H_n^{(1)}(k_0 b) \\ 0 & U_n'(b) & V_n'(b) & -k_0 H_n^{'(1)}(k_0 b) \end{bmatrix} \begin{bmatrix} A_n^{(1)} \\ A_n^{(2)} \\ A_n^{(3)} \\ A_n^{(0)} \end{bmatrix}$$

$$= \begin{bmatrix} 0 \\ 0 \\ i^n \varepsilon_n J_n(k_0 b) \\ i^n \varepsilon_n k_0 J_n'(k_0 b) \end{bmatrix}. \tag{30}$$

By solving this system and using the Wronskian identity

$$J_n(kr) H_n^{'(1)}(kr) - J_n'(kr) H_n^{(1)}(kr) = \frac{2i}{\pi kr}, \tag{31}$$

all the four coefficients $A_n^{(j)}$, $j = 0, 1, 2, 3$ are

$$A_n^{(j)} = \frac{D_j}{D}$$

with

$$D_0 = i^n \varepsilon_n \begin{vmatrix} V_n(b) & J_n(k_0 b) \\ V_n'(b) & k_0 J_n'(k_0 b) \end{vmatrix} \begin{vmatrix} h_a U_n'(a) & k_1 h_1 J_n'(k_1 a) \\ U_n(a) & J_n(k_1 a) \end{vmatrix}$$

$$+ i^n \varepsilon_n \begin{vmatrix} U_n(b) & J_n(k_0 b) \\ U_n'(b) & k_0 J_n'(k_0 b) \end{vmatrix} \begin{vmatrix} h_a V_n'(a) & k_1 h_1 J_n'(k_1 a) \\ V_n(a) & J_n(k_1 a) \end{vmatrix}, \tag{32}$$

$$D_1 = \frac{2 i^{n+1} \varepsilon_n h_a}{\pi b} \begin{vmatrix} U_n(a) & V_n(a) \\ U_n'(a) & V_n'(a) \end{vmatrix}, \tag{33}$$

$$D_2 = \frac{2 i^{n+1} \varepsilon_n h_a}{\pi b} V_n'(a) J_n(k_1 a)$$

$$- i^n \varepsilon_n k_1 h_1 V_n(a) \begin{vmatrix} J_n(k_0 b) & V_n(b) \\ k_0 J_n'(k_0 b) & V_n'(b) \end{vmatrix}, \tag{34}$$

$$D_3 = \frac{2 i^{n+1} \varepsilon_n}{\pi b} \begin{vmatrix} U_n(a) & J_n(k_1 a) \\ h_a U_n'(a) & k_1 h_1 J_n'(k_1 a) \end{vmatrix}, \tag{35}$$

$$D = \begin{vmatrix} V_n'(b) & k_0 H_n^{'(1)}(k_0 b) \\ V_n(b) & H_n^{(1)}(k_0 b) \end{vmatrix} \begin{vmatrix} h_a U_n'(a) & k_1 h_1 J_n'(k_1 a) \\ U_n(a) & J_n(k_1 a) \end{vmatrix}$$

$$+ \begin{vmatrix} U_n'(b) & k_0 H_n^{'(1)}(k_0 b) \\ U_n(b) & H_n^{(1)}(k_0 b) \end{vmatrix} \begin{vmatrix} h_a V_n'(a) & k_1 h_1 J_n'(k_1 a) \\ V_n(a) & J_n(k_1 a) \end{vmatrix}. \tag{36}$$

III. RESULTS AND DISCUSSION

The analytical solution presented in this paper involves an infinite Taylor series which must be properly truncated in practical computation; in other words, to calculate the Taylor series $R_n(r)$ in Eqs. (8), (12), and (20), terms are summed until convergent results are obtained. For all the examples computed in this study, the summation processes of $U_n(r)$ and $V_n(r)$ were stopped when

$$\frac{|U_n(r)|}{\left|\sum\limits_{n=0}^{N_1} U_n(r)\right|} < 10^{-10} \tag{37}$$

and

$$\frac{|V_n(r)|}{\left|\sum\limits_{n=0}^{N_2} V_n(r)\right|} < 10^{-10} \tag{38}$$

are satisfied, respectively. It is found that the shorter the incident waves are, the more the terms N_1 in Eq. (37) and N_2 in Eq. (38) are needed. Conversely, for the same incident wave, as the radial distance r increases, more terms are required to obtain a convergent series solution. At the same time, the outer the solutions are sought, the more the angular modes n are required.

1. Validation against Longuet-Higgins' Solutions [13]

Longuet-Higgins conducted an analytical study on wave scattering and wave energy trapping by a submerged circular sill [13]. His solution is also valid for a circular pit, where the depth can be described by Eq. (1) with $a = \infty$ and $h_0 = h_c$. To validate the present analytical solution, we set $a = 10$ m, $b = 30$ m, $h_0 = 1$ m, $h_c = 5$ m, and $s = 64$ and let h_1 increase from $1/2$ m to 5 m, then the topography approached a circular pit. The computation results for wave amplifications along the x-axis at an incident wave period of $T = 15$ s obtained by using the
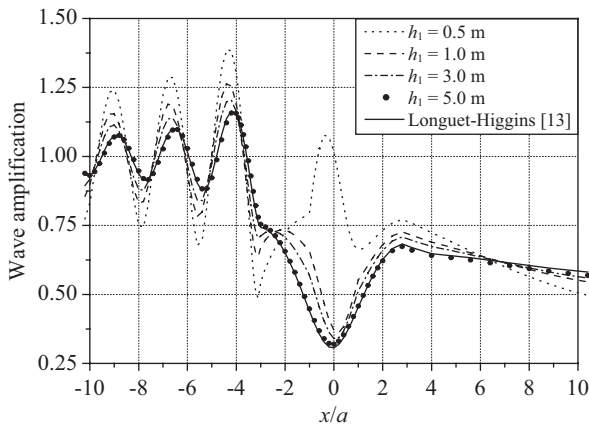
Fig. 2. **Comparison between the proposed solution and Longuet-Higgins' solution [13] for a circular pit where a = 10 m, b = 30 m, h_0 = 1 m, h_c = 5 m, s = 64, T = 15 s, and h_1 = 0.5, 1, 3, 5 m.**

present analytical model are shown in Fig. 2 along with Longuet-Higgins' classical solution for a circular pit [13]. As expected, as h_1 increased, the current analytical solutions approached Longuet-Higgins' analytical solution [13].

2. Influence of Pit Depth on Wave Amplification

This subsection details the examination of the influence of pit depth on wave amplification. As shown in Fig. 3(a), when we set the parameters a, b, h_0, h_1, and h_c and let the power exponent s decrease to 0, the pit depth h_a also decreases to 0. For T = 15 s, a = 10 m, b = 30 m, h_0 = 1 m, h_1 = 0.5 m, and h_c = 5 m and let the power exponent s decrease from s = 1/2 to s = 1/128, wave amplifications along the x-axis were calculated and shown in Fig. 3(b) along with Longuet-Higgins' analytical solution for a submerged circular sill [13]. As s decreases, namely, the pit depth h_a decreases, the amplitudes of standing waves in front of the pit decreased accordingly because of less reflection from the cylinder. Since all the values of s are less than 1, namely, the topography of the pit is convex upward, therefore, when s decreased, the amplitude in the lee side conversely increased because of less refraction from the rear wall of the pit, leading to energy scattering laterally. When s = 1/128, the present solution coincided well with Longuet-Higgins' analytical solution [13].

3. Influence of Pit Width on Wave Amplification

We subsequently investigated the influence of pit width on wave amplification. As shown in Fig. 4(a), we set the parameters a = 10 m, h_0 = 1 m, h_1 = 0.5 m, h_c = 5 m, and s = 1/2 and let the width of the pit (i.e., b) decrease from 30 m to 11 m. For T = 15 s, wave amplifications along both the x-axis and y-axis were calculated for different b and are shown in Fig. 4(b)-(c) along with Longuet-Higgins' analytical solution for a submerged circular sill [13]. When b = 30 m or $b-a$ = 20 m, the pit was the widest and the water depth was the deepest among the four cases. The large reflection from the cylinder caused high standing waves in the front side. The large
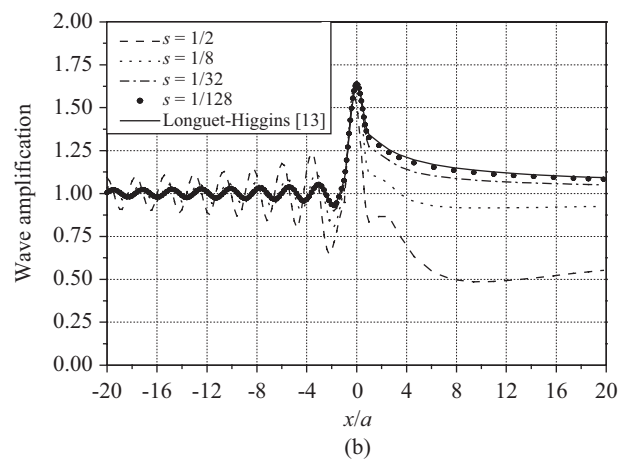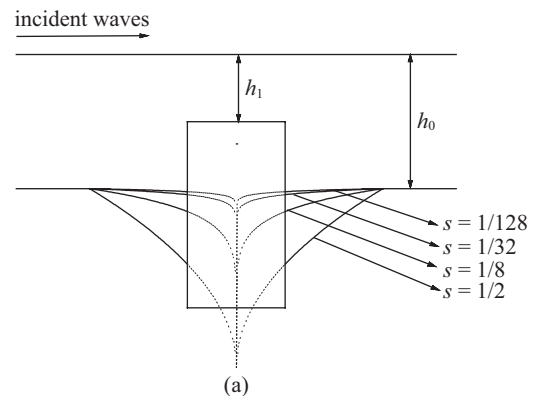

(a)

(b)

Fig. 3. **(a) Cross-sectional view along the x-axis for a cylinder mounted on a pit where a = 10 m, b = 30 m, h_0 = 1 m, h_1 = 0.5 m, h_c = 5 m, and s = 1/2, ..., 1/128. (b) Changing trend of amplifications along the x-axis for different exponents s.**

refraction from the cylinder and from the back wall of the pit caused energy to scatter laterally, leading to a local focal point of energy at y = ±4 and amplitude attenuation in the downstream. As the pit width b decreased, the pit depth h_a decreased accordingly. Thus, the changing trend of the wave amplification along x-axis was similar to that shown in Fig. 3(b). Again, when b = 11 m, the present solution approached Longuet-Higgins' analytical solution considerably well. For the case of s = 2, similar effect of the pit width on wave amplification can be observed in Fig. 5.

4. Influence of Incident Wavelength on Wave Amplification

The current analytical solution was employed to investigate wave amplification along the x-axis for various incident waves. We set a = 10 m, b = 30 m, h_0 = 1 m, h_1 = 0.5 m, and h_c = 5 m and considered two cases of s = 1/2 and s = 2. To ensure that the incident waves were in the long-wave range, we choose all the values of $k_a h_a$ in the range $0 < k_a h_a < \pi/10$, i.e., 0.05, 0.10, 0.15, 0.20, 0.25, and 0.30, where k_a is the wave number related to the deepest depth h_a. The computation results are plotted in Fig. 6(a) to (c) for s = 1/2 and in Fig. 7(a) to (c) for s = 2.
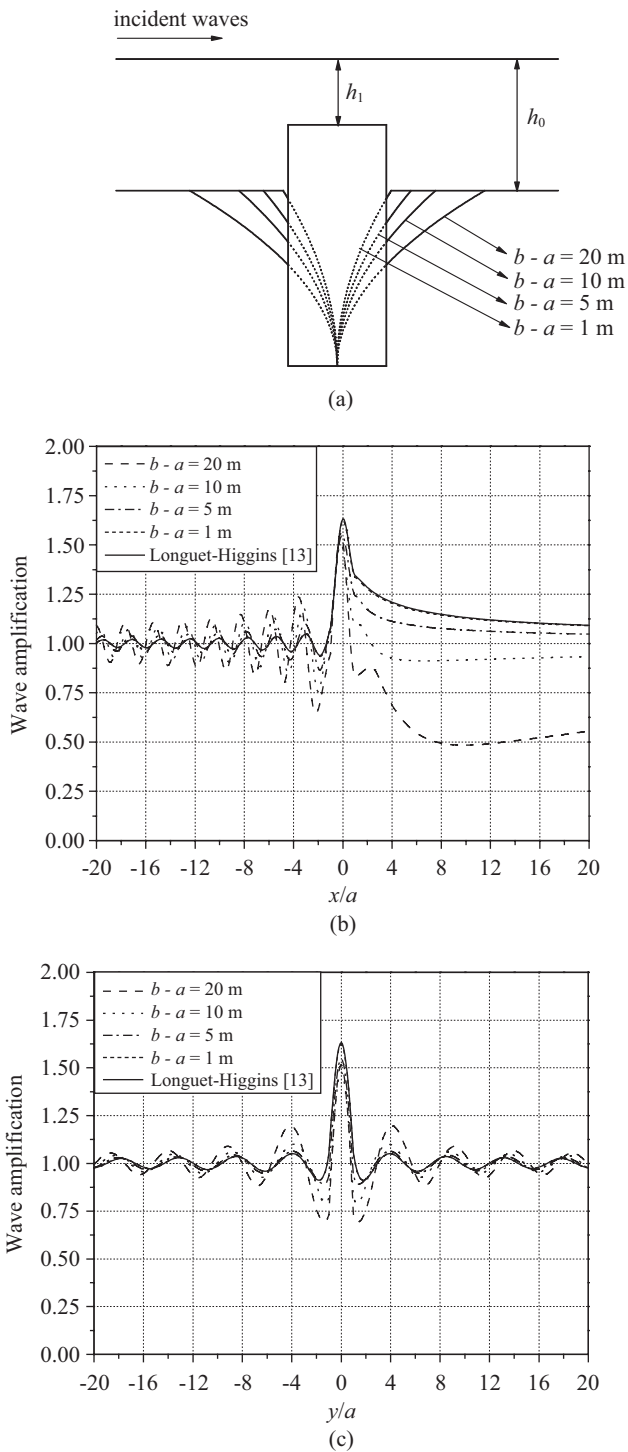
Fig. 4. (a) Cross-sectional views along the *x*-axis of a submerged cylinder mounted on an axi-symmetrical pit for which *s* = 1/2, *a* = 10 m, h_0 = 1 m, h_1 = 0.5 m, h_c = 5 m, and *b* = 30 m, 20 m, 15 m and 11 m. (b) Wave amplifications along the *x*-axis. (c) Wave amplifications along the *y*-axis.
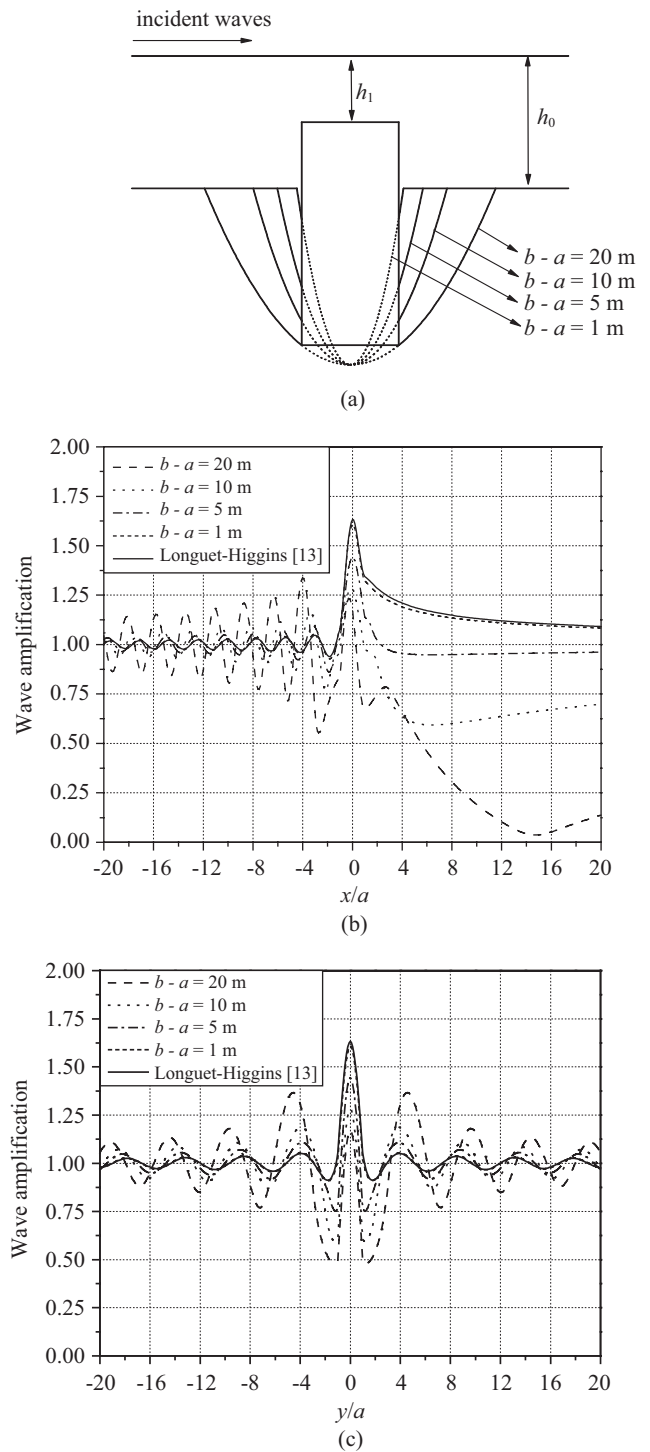
Fig. 5. (a) Cross-sectional views along the *x*-axis of a submerged cylinder mounted on an axi-symmetrical pit for which *s* = 2, *a* = 10 m, h_0 = 1 m, h_1 = 0.5 m, h_c = 5 m, and *b* = 30 m, 20 m, 15 m, 11 m. (b) Wave amplifications along the *x*-axis. (c) Wave amplifications along the *y*-axis.

Both Figs. 6(a) and 7(a) indicate that for markedly long waves (e.g., $k_a h_a$ = 0.05, 0.10), the submerged cylinder and pit impose no substantial transformation to the waves above them.

The maximal wave amplification occurred in front of the pit because of partial standing waves. As the wavelength reduced (e.g., $k_a h_a$ = 0.15, 0.20), both the reflection and refraction
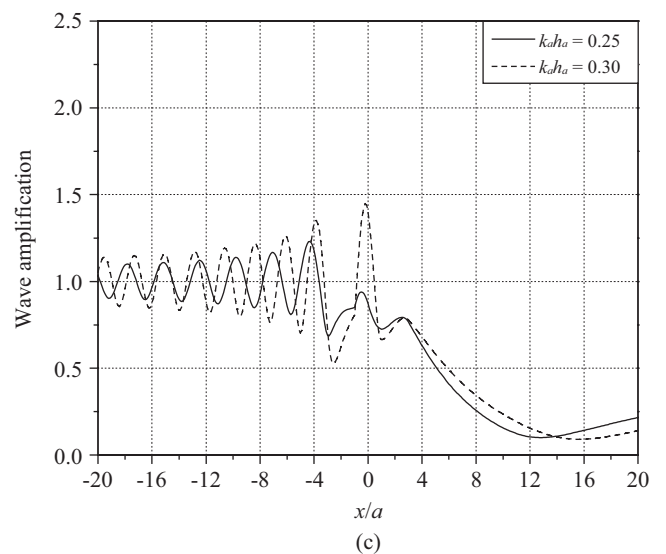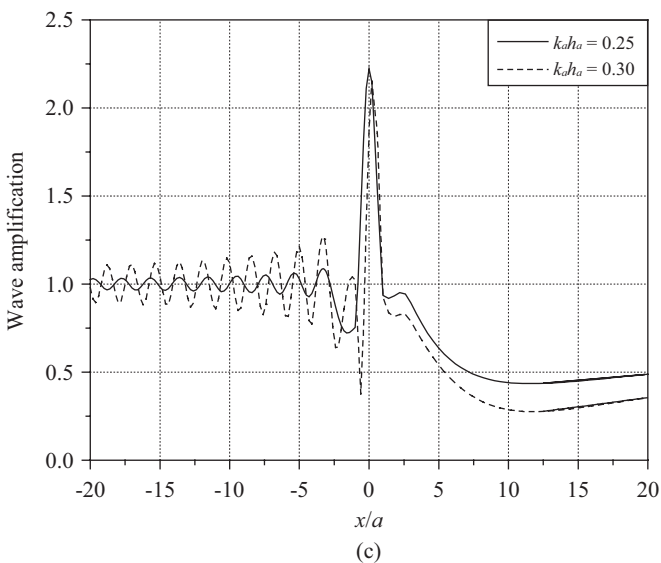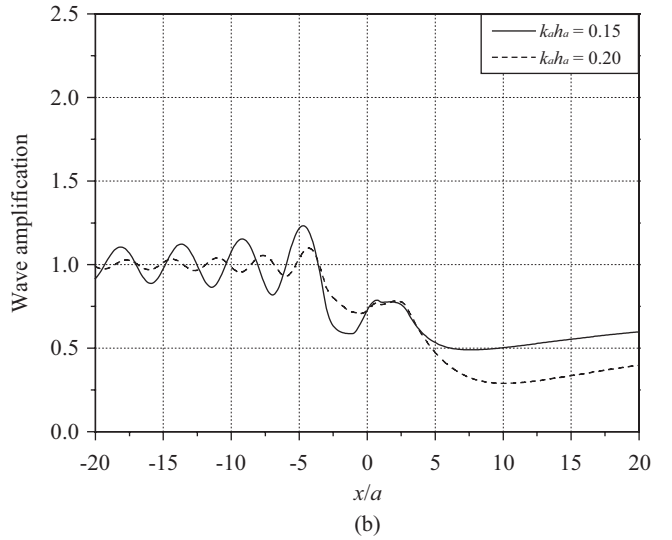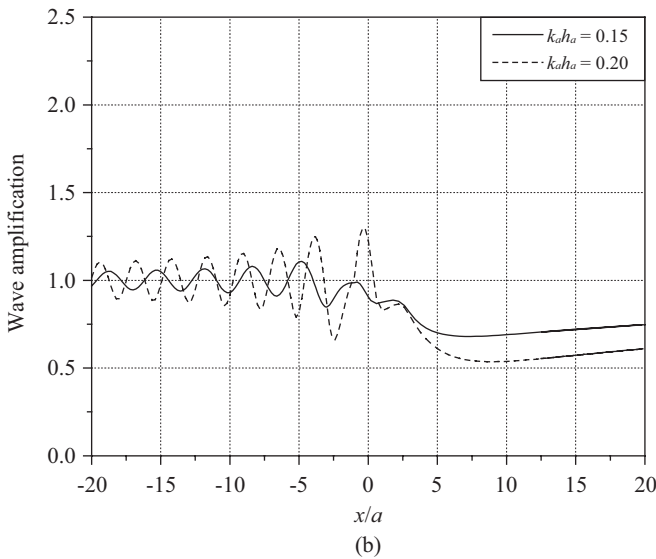
Fig. 6. Wave amplifications along the x-axis for different $k_a h_a$ with $a = 10$ m, $b = 3a$, $h_0 = 1$ m, $h_1 = 0.5$ m, $h_c = 5$ m ($h_a = 2.691$ m), and $s = 1/2$.
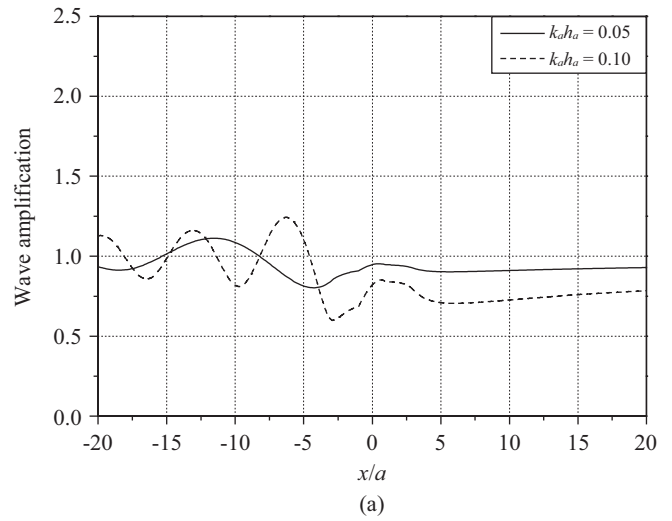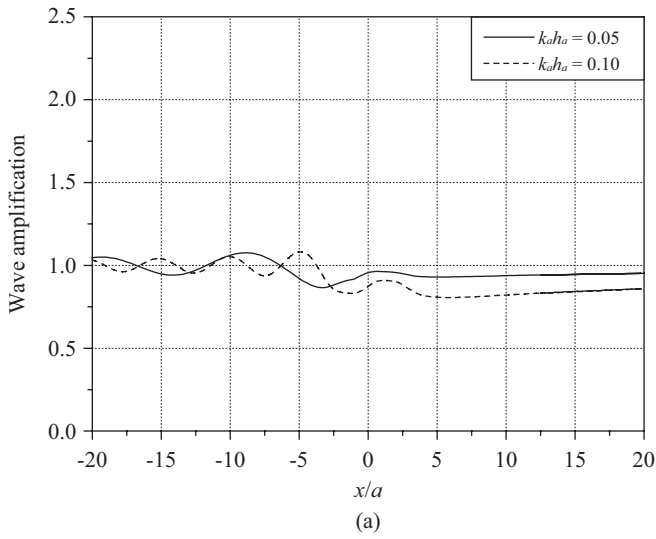

Fig. 7. Wave amplifications along the x-axis for different $k_a h_a$ with $a = 10$ m, $b = 3a$, $h_0 = 1$ m, $h_1 = 0.5$ m, $h_c = 5$ m ($h_a = 4.556$ m), and $s = 2$.

effect gradually increased in importance, and the wave could be amplified approximately 1.25 times its original amplitude in the two cases of $s = 1/2$, $k_a h_a = 0.20$, and of $s = 2$, $k_a h_a = 0.15$ some distance upstream from the cylinder centre. When the wavelength further decreased ($k_a h_a = 0.25, 0.30$), the refraction effect was markedly significant. The amplification therefore became larger, and the focal position shifted downstream to the centre of the cylinder. The amplification factor attained its maximum of more than 2 for $s = 1/2$, $k_a h_a = 0.25, 0.30$ and more than 1.4 for $s = 2$ and $k_a h_a = 0.3$.

IV. CONCLUSION

An analytical solution to the long-wave equation was derived for waves propagating over a submerged circular cylinder mounted on an axi-symmetrical pit, which may represent a submerged sill being scoured at the toes. The derived analytical solution was validated against Longuet-Higgins' classical analytical solution [13] for wave scattering and wave energy trapping by a submerged circular sill or circular pit.

On the basis of the proposed analytical solution, influences of both pit depth and width on wave amplification were intensively investigated by analysing computational results. At a fixed pit width, a deep pit causes large reflection and refraction effects. A large reflection effect leads to significant standing waves in the upstream, and a large refraction effect causes energy to scatter laterally. Thus, both the maximal wave amplification over and behind the cylinder becomes smaller. For the same reason, compared with the proposed general solution, Longuet-Higgins' classical analytical solution [13] for a circular sill with no scour pit yields the smallest amplitude of standing waves in the upstream and the largest maximal wave amplification over and behind the cylinder. These results may be useful in stability and security analysis of coastal structures because the evaluation of the scour pit size can be performed by analysing the variation in wave pattern over the cylinder-pit structure.

ACKNOWLEDGMENTS

REFERENCES

1. Homma, S., "On the behavior of seismic sea waves around circular island," *Geophysical Magazine*, Vol. 21, No. 3, pp. 199-208 (1950).

2. Hsiao, S. S., Chang, C. M., and Wen, C. C., "An analytical solution to the modified mild-slope equation for waves propagating around a circular conical island," *Journal of Marine Science and Technology*, Vol. 18, No. 4, pp. 520-529 (2010).

3. Jung, T.-H. and Lee, C., "Analytical solutions for long waves on a circular island with combined topographies," *Wave Motion*, Vol. 49, pp. 152-164 (2012).

4. Jung, T.-H., Lee, C., and Cho, Y.-S., "Analytical solutions for long waves over a circular island," *Coastal Engineering*, Vol. 57, No. 4, pp. 440-446 (2010).

5. Jung, T.-H. and Suh, K.-D., "An analytic solution to the mild slope equation for waves propagating over an axi-symmetric pit," *Coastal Engineering*, Vol. 54, No. 12, pp. 865-877 (2007).

6. Jung, T.-H. and Suh, K.-D., "An analytical solution to the extended mild-slope equation for long waves propagating over an axi-symmetric pit," *Wave Motion*, Vol. 45, No. 6, pp. 835-845 (2008).

7. Lin, P. and Liu, H.-W., "Scattering and trapping of wave energy by a submerged truncated paraboloidal shoal," *Journal of Waterway, Port, Coastal and Ocean Engineering*, Vol. 133, No. 2, pp. 94-103 (2007).

8. Liu, H.-W. and Li, Y., "An analytical solution for long-wave scattering by a submerged circular truncated shoal," *Journal of Engineering Mathematics*, Vol. 57, No. 2, pp. 133-144 (2007).

9. Liu, H.-W. and Lin, P., "An analytic solution for wave scattering by a circular cylinder mounted on a conical shoal," *Coastal Engineering Journal*, Vol. 49, No. 4, pp. 393-416 (2007).

10. Liu, H.-W., Lin, P., and Shankar, N. J., "An analytical solution of the mild-slope equation for waves around a circular island on a paraboloidal shoal," *Coastal Engineering*, Vol. 51, Nos. 5-6, pp. 421-437 (2004).

11. Liu, H.-W. and Xie, J.-J., "Discussion of 'Analytic solution of long wave propagation over a submerged hump' by Niu and Yu (2011)," *Coastal Engineering*, Vol. 58, No. 9, pp. 948-952 (2011).

12. Liu, H.-W., Xie, J.-J., and Luo, Z.-H., "Analytical solution for long-wave scattering by a circular island mounted on a general shoal," *Journal of Waterway, Port, Coastal and Ocean Engineering*, Vol. 138, No. 6, pp. 425-434 (2012).

13. Longuet-Higgins, M. S., "On the trapping of wave energy round islands," *Journal of Fluid Mechanics*, Vol. 29, Part 4, pp. 781-821 (1967).

14. MacCamy, R. C. and Fuchs, R. A., "Wave forces on piles: A diffraction theory," *US Army Corps of Engineering, Beach Erosion Board, Technical Memorandum*, Vol. 69, Washington, DC (1954).

15. Niu, X. and Yu, X., "Analytic solution of long wave propagation over a submerged hump," *Coastal Engineering*, Vol. 58, No. 2, pp. 143-150 (2011).

16. Niu, X. and Yu, X., "Analytical study on long wave refraction over a dredge excavation pit," *Wave Motion*, Vol. 48, No. 3, pp. 259-267 (2011).

17. Niu, X. and Yu, X., "Long wave scattering by a vertical cylinder with idealized scour pit," *Journal of Waterway, Port, Coastal and Ocean Engineering*, Vol. 137, No. 6, pp. 279-285 (2011).

18. Niu, X. and Yu, X., "An analytic solution for combined wave diffraction and refraction around a vertical cylinder with idealized scour pit," *Coastal Engineering*, Vol. 67, pp. 80-87 (2012).

19. Suh, K.-D., Jung, T.-H., and Haller, M. C., "Long waves propagating over a circular bowl pit," *Wave Motion*, Vol. 42, No. 2, pp. 143-154 (2005).

20. Yu, X. and Zhang, B., "An extended analytic solution for combined refraction and diffraction of long waves over circular shoals," *Ocean Engineering*, Vol. 30, No. 10, pp. 1253-1267 (2003).

21. Zhang, Y. and Zhu, S.-P., "New solutions for the propagation of long water waves over variable depth," *Journal of Fluid Mechanics*, Vol. 278, pp. 391-406 (1994).

22. Zhu, S.-P. and Zhang, Y., "Scattering of long waves around a circular island mounted on a conical shoal," *Wave Motion*, Vol. 23, No. 4, pp. 353-362 (1996).